Aircraft Emission Impacts in a Neighborhood Adjacent to a General Aviation Airport in Southern California

SHISHAN HU,[†,‡] SCOTT FRUIN,[§] KATHLEEN KOZAWA,[†,||] STEVE MARA,[||] ARTHUR M. WINER,[†] AND SUZANNE E. PAULSON*[,‡]

Department of Atmospheric and Oceanic Sciences, University of California, 405 Hilgard Ave., Los Angeles, California 90095-1565, Environmental Health Sciences Department, School of Public Health, University of California, 650 Charles E. Young Drive South, Los Angeles, California 90095-1772, Preventive Medicine, Environmental Health Division, Keck School of Medicine, University of Southern California, 1540 Alcazar Street CHP-236 Los Angeles, California 90032, and California Air Resources Board, Research Division, 1001 I Street, Sacramento, California 95814

Received April 23, 2009. Revised manuscript received August 26, 2009. Accepted September 9, 2009.

Real time air pollutant concentrations were measured downwind of Santa Monica Airport (SMA), using an electric vehicle mobile platform equipped with fast response instruments in spring and summer of 2008. SMA is a general aviation airport operated for private aircraft and corporate jets in Los Angeles County, California. An impact area of elevated ultrafine particle (UFP) concentrations was observed extending beyond 660 m downwind and 250 m perpendicular to the wind on the downwind side of SMA. Aircraft operations resulted in average UFP concentrations elevated by factors of 10 and 2.5 at 100 and 660 m downwind, respectively, over background levels. The long downwind impact distance (i.e., compared to nearby freeways at the same time of day) is likely primarily due to the large volumes of aircraft emissions containing higher initial concentrations of UFP than on-road vehicles. Aircraft did not appreciably elevate average levels of black carbon (BC), particle-bound polycyclic aromatic hydrocarbons (PB-PAH), although spikes in concentration of these pollutants were observed associated with jet takeoffs. Jet departures resulted in peak 60-s average concentrations of up to 2.2×10^6 cm^{-3}, 440 ng m^{-3}, and 30 μg m^{-3} for UFP, PB-PAH, and BC, respectively, 100 m downwind of the takeoff area. These peak levels were elevated by factors of 440, 90, and 100 compared to background concentrations. Peak UFP concentrations were reasonably correlated ($r^2 = 0.62$) with fuel consumption rates associated with aircraft departures, estimated from aircraft weights and acceleration rates. UFP concentrations remained elevated for extended periods associated particularly with jet departures, but also with jet taxi and idle, and operations of propeller aircraft. UFP measured downwind of SMA had a median mode of about 11 nm (electric mobility diameter), which was about half of the 22 nm median mode associated with UFP from heavy duty diesel trucks. The observation of highly elevated ultrafine particle concentrations in a large residential area downwind of this local airport has potential health implications for persons living near general aviation airports.

1. Introduction

A handful of studies have shown that air quality in the vicinity of major airports can be seriously impacted by emissions from activities of aircraft and ground support vehicles. Concentrations of ultrafine particle (UFP), particle-bound polycyclic aromatic hydrocarbon (PB-PAH), black carbon (BC), and NO_x were measured in the vicinity of Los Angeles International Airport (LAX) and markedly high UFP concentrations of about 5.0×10^5 cm^{-3} were observed 500 m downwind of the takeoff runways (*1*). The observed downwind UFP number concentrations were dominated by freshly generated particles with peak modes of 10−15 nm, whereas upwind UFPs were dominated by aged particles with a mode of about 90 nm. A study of London Heathrow Airport (*2*), reported aircraft NO_x at least 2.6 km from the airport. Approximately 27% of the annual mean NO_x was due to airport operations at the downwind airfield boundary, declining below 15% at 2−3 km. VOC, NO_x, CO, and CO_2 were measured around the Zurich Airport (*3*). The observed CO concentrations were highly dependent on aircraft movement, whereas NO emissions were dominated by ground support vehicles (*3*). In a study of airborne PB-PAH and vapor-phase PAH concentrations during activities of C-130H aircraft, average PB-PAH concentrations of 570 ng m^{-3} were observed 20−30 m at low and high idle, as compared to about 14 ng m^{-3} background concentrations (*4*).

Studies around general aviation airports are more limited. Recently, the South Coast Air Quality Management District made measurements of $PM_{2.5}$, total suspended particles (TSP), lead, and ultrafine particle concentrations in the areas around Santa Monica Airport (SMA), the subject of the present study, and nearby Van Nuys Airport (*5*). They found no discernible elevation of 24 h averaged $PM_{2.5}$ mass, and highly elevated total suspended particulate lead, by up to a factor of 25 (to 96 ng m^{-3}) immediately adjacent to the takeoff area and a factor of 7 higher than background (to 28 ng m^{-3}) in the residential area. They also observed spikes in ultrafine particle number concentrations associated with aircraft departures.

Typically a buffer area isolates commercial airports from residential neighborhoods to reduce noise and pollution impacts. Small airports in heavily populated areas do not necessarily have these buffers, however, so residents may be more directly exposed to aircraft emissions. In the current study, air pollutant concentrations were measured using a mobile platform (*6, 7*) during spring and summer seasons of 2008 downwind of SMA located in Santa Monica, California. SMA is a small airport operated for private aircraft and corporate jets, occupying a 1600 m by 750 m area, as shown in Figure 1. SMA is closely bounded by dense residential neighborhoods with narrow buffer areas, particularly at the ends of the runways (Figure 1). We observed markedly high concentrations of air pollutants in the residential neighborhoods downwind of SMA due to aircraft activities, particularly takeoffs, suggesting current land-use practices of reduced buffer areas around local airports may be insufficient.

* Corresponding author phone: (310)206-4442; fax: (310)206-5219; e-mail: paulson@atmos.ucla.edu.
† Department of Atmospheric and Oceanic Sciences, University of California.
‡ School of Public Health, University of California.
§ Keck School of Medicine, University of Southern California.
|| California Air Resources Board.

10.1021/es900975f CCC: $40.75
Published on Web 10/01/2009

FIGURE 1. Santa Monica Airport, nearby neighborhood residential area, and measurement sites east of SMA. The distances were measured from Google Maps.

TABLE 1. Monitoring Instruments on the Mobile Platform

instrument	measurement parameter	time resolution
TSI portable CPC, model 3007[a]	UFP count (10 nm-1um)	10 s
TSI FMPS, model 3091	UFP size (5.6−560 nm)	10 s
TSI DustTrak, model 8520[b]	$PM_{2.5}$ Mass[a]	5 s
Magee scientific aethalometer	black carbon	1 min
EcoChem PAS 2000	particle bound PAH	5 s
Teledyne API model 300E[c]	CO	20 s
LI-COR, model LI-820[c]	CO_2	10 s
Teledyne-API model 200E[c]	NO_x, NO, NO_2	20 s
Visalia sonic anemometer and temperature/RH sensor	local wind speed and direction, temperature, relative humidity (RH)	1 s
Stalker LIDAR and Vision digital system	traffic documentation, distance and relative speed	1 s

[a] The data obtained by the CPC were used only as a reference for the UFP concentrations measured by FMPS. [b] Because of concerns about the quality of this instrument's data, it is not reported here. Qualitatively, its results were consistent with the other mass-based measurements. [c] These instruments were turned off to save power for most measurement times (see text).

2. Materials and Methods

2.1. Mobile Platform and Data Collection. A Toyota RAV4 sub-SUV electric vehicle served as the mobile platform, eliminating any potential self-pollution. Table 1 shows the sampling instruments and equipment installed on the mobile platform. Ultrafine particles were measured by a fast mobility particle sizer (FMPS) spectrometer in size range of 5.6−560 nm, which includes the UFP size range of less than 100 nm. Most instruments had a time resolution of 1−20 s except the Aethalometer, which had one minute time resolution. Calibration checks and flow checks were conducted on a bimonthly and daily basis, respectively (*6*, *7*).

2.2. Measurement Sites. SMA experiences consistent wind patterns; the vast majority of days have a sea breeze (winds from the west to south-southwest) for most of the day and a land breeze at night. The runways of the airport are aligned at about 225° so that aircraft can take off into the wind. For all of our measurements, the take off direction was to the west (as is the case for at least 95% of days at SMA), with taxi and idle at the east end of the runway (Figure 1E). As the airport allows operations of nonemergency aircraft only from 07:00−23:00 on weekdays and 08:00−23:00 on weekends due to noise ordinances, only daytime hours were considered.

In the current study, the measurements were conducted primarily at four stationary sites (A−D indicating increasing distances from the airport) in the residential area downwind of the takeoff area (E) as shown in Figure 1.

Figure 1 includes a line indicating the expected centerline along which emissions plumes travel during typical on-shore flow conditions, as if it is an extension of the runways in the airport. Sites B and D were selected for measurement because they are approximately on this line. Sites A and C were chosen to test the extent of horizontal impacts and are at perpendicular distances 50 and 250 m, respectively, from the extended centerline of the runways.

In spring and summer of 2008, four days of measurements were conducted: April 14 and 20, July 20 and August 8, for 4−6 $^1/_2$ hours each day. The four stationary measurement sites in the residential neighborhoods downwind of the airport were sampled in random order to minimize systematic errors. In addition, the mobile platform was stopped briefly in the mornings and afternoons of three days (July 8, 10, and 12) in the summer season at Clarkson Rd, site B, and Barrington Ave, site D, to confirm the observations of elevated pollutant concentrations on the dedicated measurement days. The measurement times are listed in Table 2.

2.3. Data Analysis and Selection of Key Pollutants. Data were adjusted for the varying response times of the instruments on the mobile platform to synchronize the measurements (*6*, *7*). UFP, PB-PAH, and BC were selected in the current study for detailed spatial analysis because of their large concentration variations in the vicinity of SMA, and important implications for human exposure assessment. CO_2 concentrations were used in emission factor calculations (see Section 3.3.3).

3. Results and Discussion

3.1. Meteorological Data and Background Concentrations. Meteorological conditions, including temperature, relative humidity, wind speeds, and wind directions (all measured while the mobile platform was stopped), can all play a role in determining air pollutant concentrations surrounding SMA. The average wind speeds and directions are shown in Table 2 for the measurement times. The wind was stable and predominantly from the SW (204−261°) in the afternoons, with speeds of 1.9−3.0 m s^{-1}. In the mornings, the wind had lower speeds of 1.0−1.7 m s^{-1}, and variable directions in a range of 117−349°. This implies the east end of the airport was always downwind in the afternoons, but not always in the mornings, and pollutant dispersion rates were higher in the afternoons.

Average background UFP concentrations were 1.7×10^4 and 5×10^3 cm^{-3} in spring and summer of 2008, respectively. Background UFP, PB-PAH, and BC concentrations, measured on Stoner Ave 830 m NNE of the takeoff area (E), on the four dedicated days, averaged $1 \pm 0.3 \times 10^4$ cm^{-3}, 5 ± 2 ng m^{-3}, and 0.3 ± 0.1 $\mu g\, m^{-3}$, respectively, for the spring and summer measurement periods combined (PAH data was available for only two of the summer days). Measurements were made immediately preceding and/or following stops at the monitoring sites, on 12 occasions for 3−5 min each. The UFP concentrations at this site were relatively stable, consistent with an absence of aircraft or other strong UFP sources, even when there had been jet activity at SMA within the 7−8 min preceding the measurements (which happened on five

TABLE 2. Air Traffic and Meteorological Conditions during Measurements

date	time	arrivals (jets)[a]	departures (jets)[a,b]	wind speed[c] (m s^{-1})	wind direction[c]	temperature (°C)
4−14−2008	09:00−11:00	21(7)	/(3)	1.7	230	23.0
	15:30−18:00	15(8)	/(8)	2.4	235	
4−20−2008	14:00−18:00	34(13)	18(14)	2.5	261	22.0
7−08−2008	08:22−08:25	na[d]	na[d]	1.0	117	20.1
	13:20−13:46			2.2	213	21.3
7−10−2008	08:27−08:34	na[d]	na[d]	1.1	349	20.5
	13:22−13:35			1.9	204	23.8
7−12−2008	08:44−08:58	na[d]	na[d]	1.4	200	21.5
	13:24−13:34			2.1	226	24.7
7−20−2008	11:50−18:00	42(17)	20(14)	1.9	227	22.2
8−08−2008	15:30−22:00	24(9)	13(8)	3.0	237	22.2

[a] Total reported activities during the measurement time period. [b] The airport records all arrivals but only departures that exceed a specific noise threshold, thus departures exceed the values reported here. All jet departures are reported, but many small propeller plane departures are not. [c] Averaged values for the measurement periods. [d] Air traffic data are not available for these measurement periods (na).

occasions). These background values were typical of other streets around SMA away from the influence of the airport, throughout the spring and summer seasons (see also ref *6*). Sampling at sites A, B, and C, were about equally weighted between spring and summer, thus for these sites we use this combined average. Most of the sampling at site D, however, was performed during summer, so for this site we weighted the background UFP concentrations to match the distribution of sampling, and thus use 6000 cm^{-3} as the site D average background.

3.2. Air Traffic Volumes and Aircraft Operation. Air traffic logs were provided by SMA. The numbers of arriving aircraft are listed in Table 2 for the measurement periods on dedicated days. Departures are also indicated; however, the airport only recorded activity exceeding a sound threshold of 80 db at the west end of the runway, in compliance with a local ordinance, thus small propeller plane departures were not included in the log. Based on statistics of four dedicated measurement days, the number of aircraft arrivals was about 80/day, of which about 30 were various small (6−8 passengers) to large jets (20−35 passengers), and the remainder were single and twin engine piston and turboprop planes. The diurnal hourly arrival/departure aircraft activities at SMA for the four dedicated measurement days show the great majority of aircraft operations at SMA took place during 09:00−20:00 and averaged about six arrivals per hour during these hours.

Jets and propeller planes taxi 800−1000 m to the take off area E. The taxi time for aircraft is about 2 min, much longer than the acceleration time on the runway during take off, typically 20−25 s. Also, because the jet flight path from SMA intersects that of Los Angeles International Airport (LAX) about 16 km after take off, jets taking off from SMA must wait for permission from LAX, resulting in an average waiting time of about 5 min. This implies an average taxi-waiting time of about 7 min for jets departing from SMA.

3.3. Impact of SMA on Downwind Residential Area. Markedly elevated concentration peaks of ultrafine particle, PB-PAH, and BC were observed downwind of SMA, extending to at least 660 m along the wind direction (site D), and 250 m perpendicular to the prevailing wind directions (site C, about 300 m downwind). At all sampling locations, when an airplane (particularly a jet) was preparing to depart, typically a loud noise was heard first (start of taxi). If the wind was from the south-southwest to west, the noise was followed by fuel vapor odors, and then a few minutes later by elevated concentrations of ultrafine particles, black carbon, and PB-PAH. This suggests taxiing frequently produces fuel odors, while hard accelerations are usually necessary to produce large pulses of UFP, PB-PAH, or BC.

3.3.1. Average UFP Concentrations Measured Downwind of SMA. Figure 2 shows UFP concentrations at the four sites during the combined spring and summer measurement periods (Table 2). The data are for various durations at the sites, and thus the quantity of data from each site is different. The numbers of observations for sites A, B, C, and D were 730, 5100, 470, and 1700 in 5-s averages, respectively. The average UFP concentrations at sites A, B, C, and D were 106, 97, 47, and 15 K cm^{-3}, respectively, about 11, 10, 5, and 2.5 times the corresponding area background levels for all measurement days combined. Figure 2 also shows the average BC concentrations were 2.7, 1.3, 0.8, and 0.8 μg/m^3 at the sites A, B, C, and D, respectively, elevated from the area background level of 0.3 μg/m^3. PAH data are not shown because these data are not available for all days. Both UFP and BC are elevated at all four sites, consistent with airport impacts. However, they are not elevated by exactly the same ratio at each site, for reasons we are unable to explain with current data.

Site A is located in a gas station downwind of the intersection of National Blvd. and Bundy Dr. The mobile platform was stopped at the SW, upwind, corner of the gas station, and thus measurements were not likely strongly influenced by activities in the gas station. The likely small contribution of vehicles accelerating from the intersection to the observed UFP concentrations is discussed in Section 3.3.4.

3.3.2. Size Distribution and Mass of UFP Downwind of SMA. Sixty jet emission size distributions at SMA were analyzed. Aircraft emissions produced UFP with a median size mode of about 11 nm with little variability, consistent with the observations at LAX (*1*). Figure 3 shows a representative size distribution of ultrafine particles from a jet takeoff. This peak had a UFP concentration of 1.0×10^6 cm^{-3}. Figure 3 also shows a representative size distribution of UFP from an isolated heavy duty diesel truck (HDDT) measured by our MP on a surface street in the downtown area of Los Angeles. The peak UFP concentration was also about 1.0×10^6 cm^{-3}, but the mode, about 22 nm, is significantly larger than the modes of the UFP distributions observed from

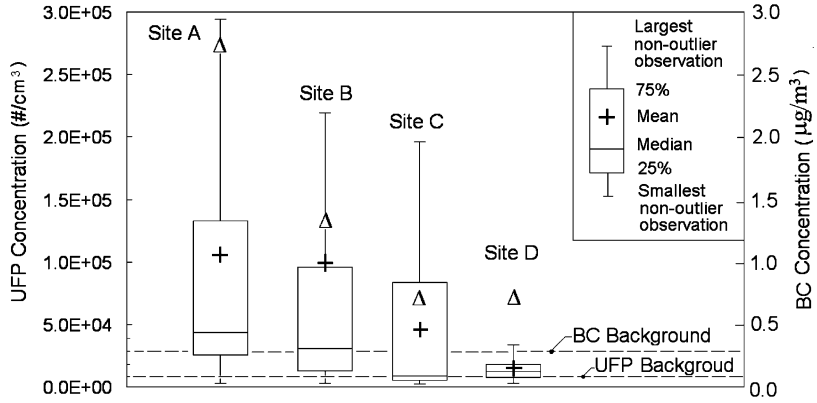

FIGURE 2. UFP concentrations at the four measurement sites during all measurement periods (Table 2). The symbol "Δ" indicates the mean value of BC concentrations for all measurement times. It is noted that because much less sampling was performed at Sites A and C, these data may carry higher uncertainties.

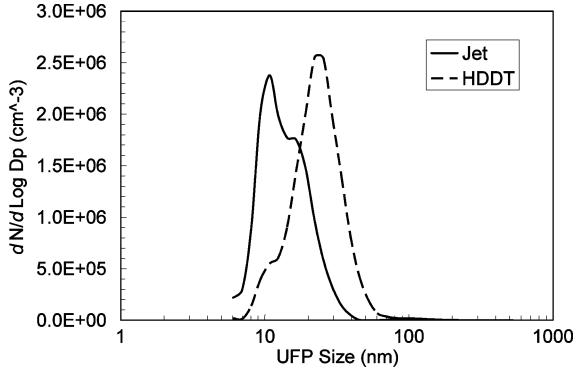

FIGURE 3. Comparison of size distribution of UFP downwind of SMA and from a heavy duty diesel truck (HDDT).

aircraft. The peak UFP concentrations from the aircraft and HDDT were about 100 and 25 times the background levels (which were not subtracted), respectively. Size distributions were collected after the emissions plumes had been diluted sufficiently that they would not be undergoing significant self-coagulation, which has been calculated to be any time after the first 1−3 s following exhaust released from the tail pipe (*8*).

Aircraft activity clearly results in markedly elevated UFP number concentrations, but because UFPs are so small, they make only modest contributions to mass concentrations. For example, the average number concentration at Clarkson site B (100 m downwind) was about 9.7×10^4 cm^{-3} during the measurement periods, 10× the area background level. The calculated mass contribution of UFP caused by aircraft averaged 0.6 μg m^{-3}, assuming a particle density of 1.2 g cm^{-3} (*1*), only about 3% of the annual basin background level of ∼18 μg m^{-3} of $PM_{2.5}$. If 24-h measurements were conducted to obtain average particle mass concentrations, the contribution of aircraft-related UFP during the aircraft operation period, typically 07:00−23:00, would be even smaller, consistent with the SCAQMD measurements (*5*). It should be noted, however, that potential health effects of UFP generally focus on the size and number of such particles and not their mass (e.g., ref *8*,).

3.3.3. Relationship between Downwind Pollutant Concentrations and Aircraft Events. Figure 4 shows typical time series of air pollutants measured at site B downwind of idle/take off area E (Figure 1) at SMA on the afternoon of July 20, 2008. On others days of measurements, similar elevated air pollutant concentrations, at least 10 times the seasonal background level, were repeatedly observed at the four sites. Note that the time of aircraft departures from the SMA log and peak UFP concentrations are very close, but do not always correspond perfectly. This may be due to occasionally high aircraft emissions during taxi as well as deviations resulting from the resolution of the airport log data (1 min), and variable travel time of the plume from the takeoff location and runway to our monitors.

Extremely high pollutant concentrations were observed at Site B, Clarkson Rd, 100 m downwind of SMA, specifically associated with jet operations at the airport. The Figure 4 time-series plot for site B shows UFP, PB-PAH, and BC as well as aircraft arrivals and some departures (upper abscissa) during the times of measurement. Here, multiple incidences of elevated air pollutant concentrations corresponded to jet departures, propeller aircraft departures, and possibly, aircraft arrivals. For example, at 12:20 (from the airport log) a Gulf Stream 4 jet (GLF4, 33 200 kg) departed, an event followed by measured concentrations of 60 s average PB-PAH and BC of 440 ng m^{-3} and 30 μg m^{-3}, respectively, resulting in elevated ratios of about 90 and 100 times the summer background levels, respectively. Both pollutants returned to background levels within about 3 min after the jet's departure. Additional spikes were observed associated with jet operations at 12:35, 12:36, 12:58, and 13:00 with 60 s average UFP concentrations up to about 2.2×10^6 cm^{-3}, about 440 times the summer background level. UFP concentrations remained elevated, hovering around 10^5 cm^{-3} for the remainder of the sampling period. The trace indicates that while arrivals of small aircraft, as well as taxi, idle, and takeoffs (although these do not appear in the log) release significant quantities of UFP, they do not appear to produce significant elevations of PB-PAH or BC.

As noted above, the average taxi and waiting of a jet before departure is about 7 min, but significantly longer taxi/waiting periods occurred from time to time. For example, during measurements at Site B, a loud noise was recorded from 12:07 until 12:20, during which time the particularly large jet (GLF4) was taxiing and waiting for take off. The peak at 12:12 and the following elevated UFP concentrations (Figure 4) were associated with this idling jet prior to its departure at 12:20. Figure 4 also shows a trace from later in the afternoon, a period with much lower aircraft activity and much lower UFP concentrations, which sometimes dropped to the summer background level of about 5000 cm^{-3} for several minutes at a time.

Significantly elevated pollutant concentrations were also observed at other three sites. For example, during one hour measurement on July 20, 2008 (13:04−14:03) at site D, just west of Barrington Ave, 660 m downwind of SMA, the UFP concentration was elevated above the summer background (5000 cm^{-3}) for most of the period, due to multiple aircraft operations (including taxi). The mean of the UFP concentration during this measurement period was 1.5×10^4 cm^{-3},

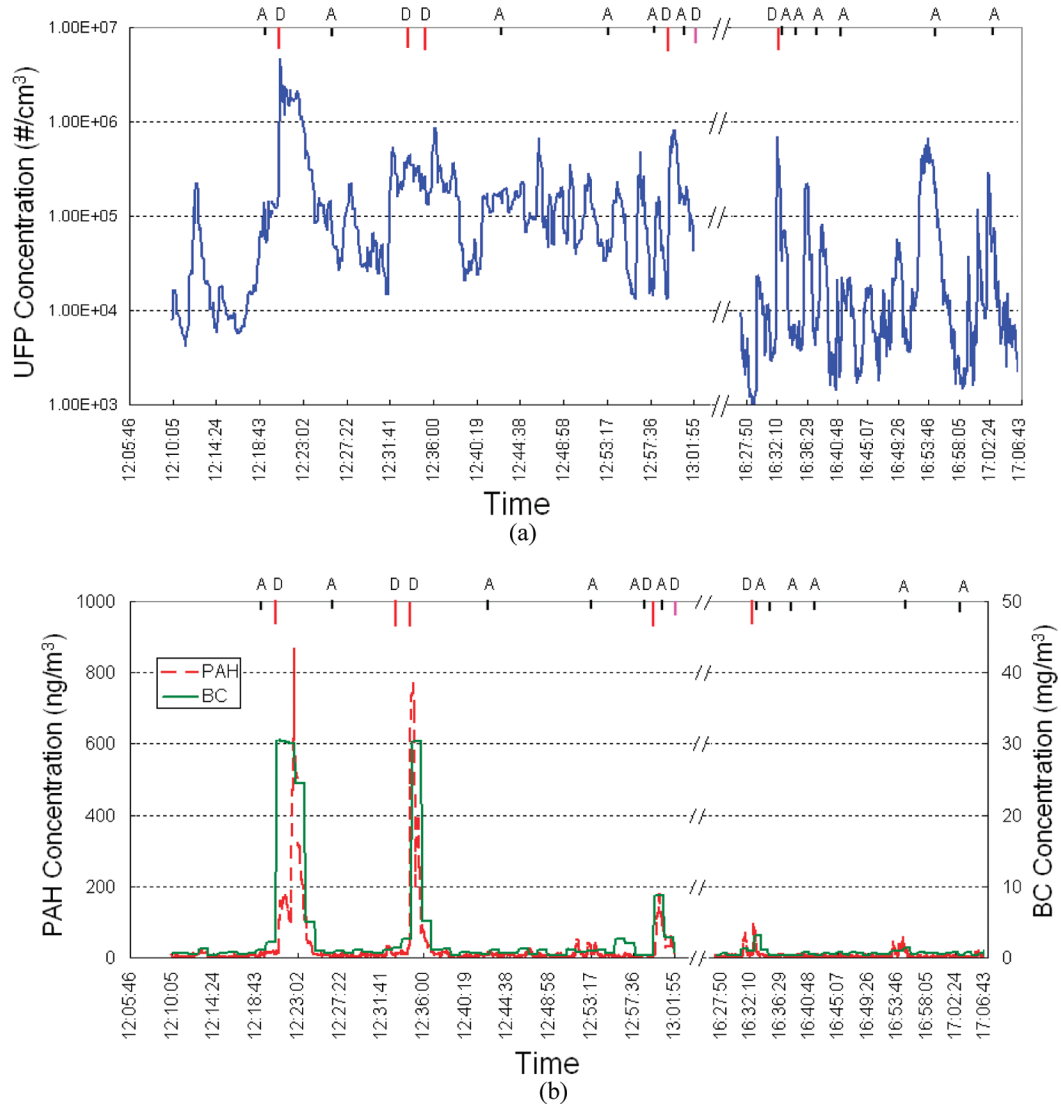

FIGURE 4. Time series plot of pollutant concentrations measured at Clarkson Rd, Site B, about 100 m downwind of the airport on July 20, 2008. (a) UFP. (b) PB-PAH and BC. On the upper abscissa, A/D denote for arrival/departure of aircraft. For departure, longer lines indicate jet activities and short lines are for activities of turboprop or piston aircraft.

about 3 times the summer background level. Spikes of PB-PAH and BC associated with aircraft activity were not observed at this site.

3.3.4. Potential Contribution from the Surface Street Immediately Downwind of the Airport. As noted earlier, a major surface street, Bundy Dr, ("Bundy", Figure 1), is located immediately east of SMA, between the usual aircraft take off area (E) and the measurement sites (A−D). To investigate the possible contribution of traffic on Bundy to elevated pollutant concentrations observed at site B, we reviewed traffic data on this street and also compared measurements made on nearby stretches of Bundy not influenced by the airport during the same sampling days as the aircraft measurements. The traffic flows on Bundy were recorded on digital video when the mobile platform was stopped at site B, and when traveling on nearby stretches of Bundy immediately preceding and following stops at the sampling sites around the SMA. The traffic counts on Bundy Dr. (and on National Blvd.) during our measurement times averaged 50−60 counts per minute, small compared to nearby freeways which have 200−300 vehicles min^{-1} during daytime. Traffic on this road is dominated by newer gasoline vehicles; further, only five heavy duty diesel trucks were encountered during 650 min of sampling on Bundy within 1.8 km of SMA.

Average on-road UFP concentrations on sections of Bundy removed from the airport impacts, but within 1800 m of SMA were much lower than observed at site B (25 m from Bundy), averaging 35 000 cm^{-3} during the sampling days listed in Table 2 (220 min of data). At site B in the absence of aircraft activity (Figure 4), the UFP concentrations were low, in the range 5000−15 000 cm^{-3}, indicating the contribution of traffic on Bundy to the average UFP measurement at site B, was less than 15 000 cm^{-3}. About one-third of the Site B UFP concentrations fell below 15 000 cm^{-3}, distributed reasonably evenly among the measurement periods. High-emitting vehicles (HEV) can cause large spikes of UFP concentrations, over 10^6 cm^{-3}, but these vehicles were rare (above). Vehicle-related UFP spikes are also brief, lasting less than 30 s for solo vehicles, and even shorter times in traffic. Hence, the contributions of high emission vehicles on Bundy to the average UFP concentrations measured at Site B were small, and HEV are unable to explain the frequent elevated UFP lasting 2 min or longer (e.g., Figure 4a) observed at the site B. This reinforces that the elevated pollutant concentrations we measured at site B were due to the emissions from aircraft at SMA. Similarly, we believe the elevated UFP concentration measured at site A in the gas

TABLE 3. Information about Aircraft Active at SMA

	code	type	passengers	weight (kg)	takeoff distance (m)	takeoff IAS (m s^{-1})[a]	associated peak UFP concentration (no. cm^{-3})
1	BE36	piston	6	1650	350	50	1.0×10^5
2	BE58	piston	4−5	2500	700	65	2.5×10^5
3	BE40	small jet	6−8	7300	1200	80	3.6×10^5
4	C152	piston	1	760	220	44	8.5×10^4
5	C441	turboprop	9	4470	550	65	1.2×10^5
6	C550	small jet	6	6850	1000	75	3.4×10^4
7	C560	small jet	8	7210	963	65	7.3×10^5
8	C750	large jet	12	16193	1740	80	1.8×10^6
9	F2TH	large jet	9−19	16240	1600	75	1.3×10^6
10	H25B	mid jet	8−14	12430	1700	75	6.6×10^5
11	LJ35	small jet	6−8	8300	1300	87	1.6×10^5
12	E135	large jet	35	19990	1400	82	
13	GLF4[b]	large jet	14−19	33200	1600	90	4.6×10^6

[a] Indicated aircraft speed; the speed as the aircraft leaves the ground. [b] Peak UFP concentration of GLF4 shown here was not included in the correlation because its fuel consumption rate estimated from eq 4 (see text) was an outlier from the cluster of values for other aircraft.

station was dominated by aircraft, not by vehicle emissions from the intersection of Bundy Dr. and National Blvd.

3.3.5. Comparison of Impact Areas from Santa Monica Airport and Freeways during Daytime. Measurements made in Southern California (*6, 9*) indicated UFP and other vehicle-related pollutant concentrations return to background by about 300 m downwind of major roadways during daytime, although the impact distance is much greater prior to sunrise (*6*). In the current study, average UFP concentrations 660 m downwind of SMA during the daytime were about 2.5× (all data) and 3× (summer only) the background, indicating a much greater impact distance for the airport than for roadways. Similar to our observation, elevated UFP concentrations were observed 900 m downwind of a runway at Los Angeles International airport (*1*). The phenomenon was attributed to landing aircraft passing within a few hundred meters overhead, combined with incomplete dilution of the high numbers of UFP emitted from aircraft during takeoff.

We believe the relatively long impact distance downwind of SMA, further than 660 m, is a result of the higher initial concentrations of UFP in aircraft emissions, combined with their larger volumes relative to vehicles. As far as we are aware, studies of particle emissions directly from aircraft are limited to large jets. We estimated UFP emissions per kg of fuel consumed from the jet aircraft operated at SMA for cases where we observed departures that produced clear isolated spikes in both CO_2 and UFP. Two suitable isolated peaks observed at the stop at site B on August 8 indicate the aircraft emissions contained roughly 5×10^{16} particles/kg of fuel consumed. The CO_2 difference was 12 ± 1.5 ppm, and the UFP difference was $(3.7 \pm 0.5) \times 10^5$ particles cm^{-3}. Large aircraft emissions have been reported to contain a range of $0.3-5 \times 10^{16}$ particles/kg of fuel consumed (*10, 11*). Our estimate for SMA is at the high end of this range. Also for commercial gas turbines, high particle numbers have been reported at lower thrust levels associated with lower fuel consumption rates (*10*), suggesting that even with much lower fuel consumption rates, aircraft taxi, and idle may be a significant source of UFP.

Our UFP emissions estimates for aircraft at SMA are 16−100 times higher than UFP emitted per kg of fuel consumed by light duty vehicles ($5 \times 10^{14}-3 \times 10^{15}$ particles/kg) (*12, 13*) and 5−8 times higher than heavy duty vehicles ($6 \times 10^{15}-1 \times 10^{16}$ particles/kg) (*12, 14*). Although the on-road vehicle values were measured under a range of typical on road conditions, and thus are not directly comparable to our aircraft measurements which are dominated by idle/low load and maximum load conditions, they are each real-world estimates relevant to exposure assessment.

Aircraft fuel consumption rates during takeoff are roughly 50−300 g s^{-1} for small piston or turboprop planes and can be up to about 500−5000 g s^{-1} for the types of jets that operate at SMA (*15*), much higher than rates for motor vehicles of 1−10 g s^{-1}. The fuel consumption rates for jets during takeoff tend to be high (up to several times those during cruise) because the jet engines are designed for high speeds and at high altitudes. This means aircraft emissions, especially during takeoff, have much higher volumetric flow rate than that of motor vehicles. This large volume of high concentration aircraft emissions is expected to take longer to be dissipated and diluted to the background level than vehicle emissions on roadways, consistent with our observations.

Zhang and Wexler proposed a model of aerosol dilution near roadways (*8*). They suggested a dilution ratio of about 1000:1 is complete in the first 1−3 s during the "tailpipe-to-road" stage, and an additional 10:1 dilution is completed in the following 3−10 min, the "road-to-ambient" stage. Dilution of aircraft emissions at the SMA are also complicated by the topography immediately east of SMA. The takeoff area is about 9 m higher than the measurement site B. Aircraft emissions need to first pass over a fence, about 3.5 m high, designed to mitigate noise and emissions impacts on neighborhoods, and then to pass over Bundy Dr to move into the downwind residential neighborhoods.

The travel times for pollutants to site B, and from the site B to D were 17−50 s and 1.5−6 min (corresponding to wind speeds of 2−6 m s^{-1}), in the range of the wind-shear-dominated second stage "road- to-ambient" dilution period (*8*). This implies a dilution ratio at site B vs site D of 10:1 or less. The average summer UFP concentrations at sites B and D were 8.9×10^4 and 1.5×10^4 cm^{-3}, respectively, indicating a dilution factor of about 8, for summer background concentrations of about 5000 cm^{-3}. This dilution factor is consistent with our estimates above, implying that the larger downwind impact area of the airport compared to that of roadways results from the large volumetric pulse of high concentration emissions produced by aircraft.

3.3.6. Correlation of Site B UFP Concentration and Estimated Aircraft Fuel Consumption Rates. To compare measured UFP concentrations with airport activities, we estimated aircraft fuel consumption rates at take off. Aircraft weight (m), passenger number, activity type (departure/arrival), take off length (L), and indicated aircraft speed (U, the aircraft velocity leaving the ground), determine the fuel consumption rate of ($\dot{m}_{fuel}$) during take off. Values for m, L, and U were obtained from aircraft specifications. Passengers, crew, and luggage usually add 6−15% of aircraft weight. If

a constant acceleration rate of aircraft on the runway is assumed,

$$L = at^2/2 \quad (1)$$

$$U = at \quad (2)$$

$$m_{\text{fuel}} \propto mU^2C_0C_1/2 \quad (3)$$

Here, a is the aircraft acceleration rate on the runway; t is the time of aircraft spent on the runway during acceleration; m_{fuel} is the total fuel mass consumed by aircraft during acceleration; C_0 is the overall conversion efficiency of energy from fuel to aircraft kinetic, and C_1 is a constant accounting for the weight of the passengers, crew, and luggage. Here, the same C_0 and C_1 are assumed for all aircraft. Combining eqs 1−3, we obtain a fuel consumption rate for aircraft during acceleration on the runway as:

$$\dot{m}_{\text{fuel}} \propto mU^3/L \quad (4)$$

For similar atmospheric conditions and assuming the same dilution ratio of emissions from all aircraft, the peak UFP concentrations measured at site B should be roughly proportional to the peak air pollutant concentrations emitted from an aircraft, which are proportional to the fuel consumption rate during take off. The jets at SMA are heavier (7000−33 000 kg), faster (indicated aircraft speed, or IAS, of 70−90 m s^{-1}), and have longer take off lengths (1000−1800 m) than propeller aircraft. The calculated $\dot{m}_{\text{fuel}}$ was 5−10 times larger for jets than propeller planes.

Reasonable correlations were observed between the measured peak UFP concentrations at site B and the parameter mU^3/L for aircraft departures associated with spikes in UFP concentrations measured at site B. The measured UFP concentrations and the associated aircraft code, type, weight, takeoff distance, and takeoff speed, are listed in Table 3. The squared Pearson correlation coefficient (r^2) of 0.62 indicates UFP emissions and hence concentrations are reasonably related to aircraft fuel consumption rate. In general, larger aircraft are associated with higher emissions and downwind concentrations of UFP.

Acknowledgments

We acknowledge support for this study by the California Air Resources Board, Contract No. 04-348. We express our appreciation to Drs. Jorn Herner and Ying-Kuan Hsu, and Dane Westerdahl of ARB for their assistance. We also thank Hwajin Kim at UCLA, Prof. Neil Humphrey at the University of Wyoming, Maria Dacanay at The City of Santa Monica, and Dr. Rod Merl and Mr. Stelios Makrides at Santa Monica Airport for their contributions to the study, and Dr. P.M. Fine of the South Coast Air Quality Management District for sharing his unpublished results.

Literature Cited

(1) Westerdahl, D.; Fruin, S.; Fine, P. L.; Sioutas, C. The Los Angeles international airport as a source of ultrafine particles and other pollutant to nearby communities. *Atmos. Environ.* **2008**, *42*, 3143–3155.
(2) Carslaw, D. C.; Beevers, S. D.; Ropkins, K.; Bell, M. C. Detecting and quantifying aircraft and other on-airport contributions to ambient nitrogen oxides in the vicinity of a large international airport. *Atmos. Environ.* **2006**, *40*, 5424–5434.
(3) Schürmann, G.; Schäfer, K.; Jahn, C.; Hoffmann, H.; Bauerfeind, M.; Fleuti, E.; Rappengluck., B. The impact of NO_x, CO and VOC emissions on the air quality of Zurich airport. *Atmos. Environ.* **2007**, *41*, 103–118.
(4) Childers, J. W.; Witherspoon, C. L.; Smith, L. B.; Pleil, J. D. Real-time and integrated measurement of potential human exposure to particle-bound polycyclic aromatic hydrocarbons (PAHs) from aircraft exhaust. *Environ. Health Perspect.* **2000**, *108*, 853–862.
(5) Fine, P. M. *Community-Scale Air Toxics Monitoring—sun Valley Neighborhood and General Aviation Airport*; U.S. EPA Air Toxics Data Analysis Workshop Presentation: Chicago, IL, 2007.
(6) Hu, S.; Fruin, S.; Kozawa, K.; Mara, S.; Paulson, S. E.; Winer, A. M. A wide area of air pollutant impact downwind of a freeway during pre-sunrise hours. *Atmos. Environ.* **2009**, *43*, 2541–2549.
(7) Kozawa, K. H.; Fruin, S. A.; Winer, A. M. Near-road air pollution impacts of goods movement in communities adjacent to the ports of Los Angeles and Long Beach. *Atmos. Environ.* **2009**, *43*, 2960–2970.
(8) Zhang, K. M.; Wexler, A. S. Evolution of particle number distribution near roadways-Part I: analysis of aerosol dynamics and its implications for engine emission measurement. *Atmos. Environ.* **2004**, *38*, 6643–6653.
(9) Zhu, Y.; Hinds, W. C.; Kim, S.; Shen, S.; Sioutas, C. Study of ultrafine particles near a major highway with heavy-duty diesel traffic. *Atmos. Environ.* **2002b**, *36*, 4323–4335.
(10) Lobo, P.; Hagen, D. E.; Whitefield, P. D.; Aloes, D. J. Physical characterization of aerosol emissions from a commercial gas turbine engine. *J. Propul. Power* **2007**, *23*, 919–929.
(11) Herndon, S. C.; Onasch, T. B.; Frank, B. P.; Marr, L. C.; Jayne, J. T.; Canagaratna, M. R.; Grygas, J.; Lanni, T.; Anderson, B. E.; Worsnop, D.; Miake-Lye, R. C. Particulate emissions from in-use commercial aircraft. *Aerosol Sci. Technol.* **2005**, *39*, 799–809.
(12) Kirchstetter, T. W.; Harley, R. A.; Kreisberg, N. M.; Stolzenburg, M. R. On-road measurement of fine particle and nitrogen oxide emissions from light- and heavy-duty motor vehicles. *Atmos. Environ.* **1999**, *33* (18), 2955–2968.
(13) Geller, M. D.; Sardar, S. B.; Phuleria, H.; Fine, P. M.; Sioutas, C. Measurements of particle number and mass concentrations and size distributions in a tunnel environment. *Environ. Sci. Technol.* **2005**, *39* (22), 8653–8663.
(14) Westerdahl, D.; Wang, X.; Pan, X.; Zhang, K. M. Characterization of on-road vehicle emission factors and microenvironmental air quality in Beijing, China. *Atmos. Environ.* **2009**, *43*, 697–705.
(15) Humphrey, N. F. Personal communication. 2009.

ES900975F